

Stage-Aware Context Assembly for Long-Context Memory Retrieval

Clement Deust
Independent Researcher
github.com/cdeust/Cortex

May 2026

Abstract

Dense vector retrieval degrades structurally at scale. On BEAM [Tavakoli et al., 2026], the hardest publicly available long-context memory benchmark at 10 million tokens per conversation, a production-grade 5-signal fusion pipeline with cross-encoder reranking drops from 0.591 MRR at 100K tokens to 0.353 MRR at 10M tokens—a 40% degradation that no amount of reranking or embedding model upgrade can address because the failure is geometric, not parametric. We present a structured context assembly architecture that recovers this degradation: a two-primitive system combining (1) a priority-budgeted prompt decomposer with domain-aware condensers and truncation warning injection, and (2) a stage-aware assembler (two phases implemented and evaluated; a third summary-fallback phase is designed but not yet benchmarked) with submodular coverage selection, Personalized PageRank entity graph traversal, and schema-structured summary fallback. On BEAM-10M (196 questions, 10 conversations), the assembler with ground-truth stage boundaries (BEAM `plan_id`) achieves 0.429 MRR, a +21.5% improvement over the flat baseline (0.353), with 8 of 10 memory abilities improving. Replacing the oracle labels with *label-free* temporal stage detection (day-level timestamp partitioning, no metadata) raises this to 0.471 (+33.4%): temporal proximity proved a stronger stage signal than topic boundaries on this benchmark (§6.3), so the architecture deploys without oracle metadata (§8.7). The architecture was originally designed in September 2025 for generating coherent product requirement documents on Apple Intelligence’s 4,096-token context window—one month before the BEAM paper was published. The key insight is that at scale, structured composition of what enters context outperforms improving how individual items are retrieved. Code, data, and benchmark harness are publicly available.¹

1 Introduction

Retrieval-augmented generation (RAG) has become the dominant paradigm for grounding language models in external knowledge. The standard recipe—embed documents, index them in a vector store, retrieve the top- k nearest neighbors at query time, and concatenate them into the prompt—works well when the corpus is moderate and topically diverse. But when applied to long-term conversational memory, where a single user’s history spans millions of tokens of thematically overlapping content, this recipe fails in a specific and well-characterized way.

¹<https://github.com/cdeust/Cortex>

1.1 The Scaling Failure

Consider a memory system storing the conversational history of a software developer over six months. At 100K tokens (~ 94 memories), the content is sparse enough that a dense retrieval query returns meaningfully different candidates. At 10M tokens ($\sim 7,500$ memories), the content has accumulated around a small number of recurring topics—the same frameworks, the same debugging patterns, the same architectural decisions discussed from slightly different angles across hundreds of sessions. The embedding space becomes crowded with near-identical vectors, and top- k retrieval degenerates into returning k paraphrases of the same piece of information.

This is not a failure of any particular embedding model. Three well-documented phenomena make it structural:

Hubness [Radovanović et al., 2010]. In high-dimensional spaces, certain points become disproportionately frequent nearest neighbors of many queries. Formally, let $N_k(x)$ denote the number of times point x appears in the k -nearest-neighbor lists of all other points. In uniformly distributed data, $\mathbb{E}[N_k(x)]$ is constant, but the variance of N_k grows with dimensionality. The skewness of the N_k distribution—the *hubness*—increases monotonically with $d/\log n$ where d is the dimensionality and n is the sample size. Radovanović et al. [2010] showed that this is an inherent property of the geometry, not an artifact of particular distance metrics. As corpus size grows, a small set of “hub” memories dominates the top- k results regardless of query content. At 7,500 memories in 384 dimensions, we observe empirically that the top-5 retrievals for topically distinct queries share 2–3 common memories—the hubs. These hub memories are not necessarily irrelevant; they are typically the most “central” memories that have high average similarity to all queries. But their dominance crowds out the specific, targeted memories that would actually answer the query.

Concentration of distances [Beyer et al., 1999]. As dimensionality grows relative to sample size, the ratio of the nearest-neighbor distance to the farthest-neighbor distance converges to 1. Formally, for i.i.d. points drawn from any distribution with finite variance:

$$\lim_{d \rightarrow \infty} \Pr \left[\frac{\|X_{\max} - q\| - \|X_{\min} - q\|}{\|X_{\min} - q\|} \leq \epsilon \right] = 1 \quad (1)$$

for any $\epsilon > 0$. The practical consequence: in 384 dimensions with 7,500 points, the gap between the “most relevant” and “50th most relevant” memory shrinks to the point where cosine similarity cannot reliably discriminate them. Adding more dimensions helps, but the next phenomenon places a lower bound on how many dimensions suffice.

Dimensionality lower bounds [Larsen and Nelson, 2017]. The Johnson–Lindenstrauss lemma guarantees that pairwise distances among n points can be preserved to within $(1 \pm \epsilon)$ in $O(\epsilon^{-2} \log n)$ dimensions. Larsen and Nelson [2017] proved this is tight: any embedding that preserves pairwise distances among n points to within $(1 \pm \epsilon)$ requires $\Omega(\epsilon^{-2} \log n)$ dimensions. For $n = 7,500$ and $\epsilon = 0.1$ (10% distance preservation), this gives:

$$d \geq \frac{1}{\epsilon^2} \cdot \ln(n) = \frac{1}{0.01} \cdot \ln(7500) \approx 100 \cdot 8.92 \approx 892 \quad (2)$$

Our 384-dimensional embeddings (all-MiniLM-L6-v2) operate below this lower bound, meaning pairwise distance preservation to 10% accuracy is not guaranteed even in principle for 7,500 points.

We note this is a lower bound on *pairwise-distance* preservation, not on nearest-neighbor *ordering*, which can be preserved below the JL bound; we cite it as indicative of the regime, not as a

proof that retrieval must fail at 384 dimensions. The empirical degradation in Table 7 is the actual evidence.

The consequence is measurable. On the BEAM benchmark [Tavakoli et al., 2026], our production Weighted Reciprocal Rank Fusion (WRRF) pipeline—which fuses five PostgreSQL-side signals (vector similarity, full-text search, trigram matching, thermodynamic heat, temporal recency) with client-side FlashRank cross-encoder reranking—scores:

- **BEAM-100K** (94 memories/conversation): 0.591 MRR
- **BEAM-10M** (7,500 memories/conversation): 0.353 MRR

A 40% degradation at 100× scale. No reranking layer, query rewriting strategy, or embedding model upgrade addresses a geometric ceiling. The architecture must change.

1.2 The Insight

The insight behind this work is that the problem is not *how* to retrieve better, but *what* to compose into context. A flat retrieval pipeline treats the context window as a ranked list: the top- k most similar items, concatenated. A structured assembly pipeline treats the context window as a *document* with typed sections, priority ordering, and explicit awareness of what was included and what was cut.

This distinction matters most when the corpus is large and thematically dense—precisely the regime where flat retrieval fails. By partitioning the corpus into topical stages, retrieving within the current stage first, following entity graph connections to related stages, and falling back to summaries for uncovered stages, the assembler recovers information that flat top- k cannot reach.

The analogy is to how humans prepare for a meeting: you do not read every email from the past year sorted by relevance score. You identify the current topic, gather the directly relevant material, follow references to related discussions, and glance at summaries of background context. The structured approach is not better because it uses a superior search algorithm—it is better because it organizes the search into scopes that match the information need.

1.3 Origin

This architecture did not originate from a retrieval research project. It was designed in September 2025 for a production Swift application (`ai-architect-prd-builder`) that generates comprehensive product requirement documents using Apple Intelligence, which has a 4,096-token context window. The application must produce coherent 9-page documents with cross-referenced requirements, working code examples, verification reports, and Jira ticket specifications—none of which fit in the model’s context simultaneously.

The solution: *do not try to fit everything. Structure what goes in, prioritize it, and tell the model what was cut.*

This principle—born from a practical constraint on a tiny context window—turns out to be exactly what is needed for 10-million-token memory retrieval. The problem is structurally identical at both scales: the available context is smaller than the relevant information, so you must be intelligent about what enters the context.

1.4 Contributions

We make four contributions:

1. **ContextDecomposer**: a priority-budgeted prompt assembly primitive with typed placeholder slots, domain-aware condensers, progressive condensation, and truncation warning injection—a design contribution we found undescribed in the 2024–2026 retrieval, prompt engineering, or agent memory literature we surveyed, and whose effect on answer quality we do not evaluate here.
2. **StageAwareContextAssembler**: a hierarchical retrieval architecture (two phases evaluated; third designed) with a configurable budget split (default 60/30/10, where the 10% is reserved for the designed-but-unwired summary-fallback phase), combining submodular coverage selection [Krause and Guestrin, 2008], Personalized PageRank entity graph traversal [Gutierrez et al., 2024], and schema-structured summary fallback [Tse et al., 2007].
3. **Empirical validation** on BEAM at two scales (100K and 10M tokens), showing that structured assembly is net-flat at small scale (where flat retrieval is already sufficient) and provides a +21.5% improvement at large scale with oracle stage labels, rising to +33.4% with label-free temporal stage detection (where flat retrieval collapses)—with 8 of 10 memory abilities improving in both configurations.
4. **Ablation analysis** isolating the contribution of submodular selection (+17.6% over naive top- k) and establishing that the architecture’s value is compositional rather than attributable to any single mechanism.

1.5 Paper Organization

Section 2 reviews related work across dense retrieval, long-context memory systems, hierarchical retrieval, and the biological foundations that informed design choices. Section 3 presents the method in detail, including the ContextDecomposer algorithm, the three-phase assembler, and the integration with the existing Cortex pipeline. Section 4 describes the experimental setup, benchmarks, baselines, and measurement protocol. Section 5 presents results at both scales with per-ability breakdowns. Section 6 provides analysis of scale-dependent behavior, the multi-session reasoning sign flip, and comparison with published systems. Section 7 documents the provenance timeline with verifiable commit SHAs. Section 8 discusses limitations and future work. Section 9 concludes.

2 Background and Related Work

2.1 Dense Retrieval at Scale

The standard dense retrieval pipeline embeds queries and documents into a shared vector space and retrieves by nearest-neighbor search. The bi-encoder architecture [Karpukhin et al., 2020, Reimers and Gurevych, 2019] maps queries and passages independently, enabling pre-computation of passage embeddings and sublinear retrieval via approximate nearest-neighbor indices (HNSW, IVF, product quantization).

Benchmarking dense retrieval. BEIR [Thakur et al., 2021] established zero-shot evaluation across 18 diverse datasets, revealing that dense retrievers trained on MS MARCO generalize poorly to domain-specific corpora. MTEB [Muennighoff et al., 2023] extended this to 56 datasets across 8 tasks, becoming the standard benchmark for embedding models. Both benchmarks evaluate on corpora where documents are topically diverse—web pages, Wikipedia passages, scientific abstracts, and forum posts.

Long-document retrieval. LongEmbed [Zhu et al., 2024] extends evaluation to documents exceeding 8,000 tokens, testing whether embedding models preserve relevance over longer passages. However, it still assumes a diverse corpus: the challenge is encoding long documents, not discriminating among thousands of topically similar documents from a single user.

The gap in existing benchmarks. The failure mode we address—topical density within a single user’s conversational history, where 7,500 memories discuss overlapping topics in similar vocabulary—is not covered by existing retrieval benchmarks. LongMemEval [Wu et al., 2025] evaluates conversational memory but at modest scale ($\sim 115\text{K}$ tokens, ~ 40 sessions). LoCoMo [Maharana et al., 2024] tests multi-hop and adversarial queries but caps at 10 conversations. BEAM is the first benchmark to stress-test memory retrieval at 10M tokens per conversation, and the results confirm that existing systems collapse at this scale: the best published system (LIGHT with Llama-4-Maverick) achieves only 0.266.

2.2 Reciprocal Rank Fusion and Hybrid Search

Our baseline, Weighted Reciprocal Rank Fusion (WRRF), extends the original Reciprocal Rank Fusion [Cormack et al., 2009] with per-signal weights. Given m ranking signals, the fused score for document d is:

$$\text{WRRF}(d) = \sum_{i=1}^m \frac{w_i}{k + r_i(d)} \quad (3)$$

where $r_i(d)$ is the rank of d under signal i , k is a smoothing constant (we use $k = 60$, following the original RRF recommendation), and w_i is the weight for signal i .

Cortex’s WRRF pipeline fuses five signals:

Table 1: WRRF signal configuration.

Signal	Weight	Computed At
Vector similarity (pgvector HNSW, 384D)	0.35	PostgreSQL
Full-text search (tsvector, BM25-weighted)	0.25	PostgreSQL
Trigram matching (pg_trgm)	0.15	PostgreSQL
Thermodynamic heat (access recency/frequency)	0.15	PostgreSQL
Temporal recency (exponential decay)	0.10	PostgreSQL

All five signals are computed server-side in a single PL/pgSQL stored procedure (`recall_memories()`), returning pre-fused results. Client-side, FlashRank (ONNX cross-encoder) reranks the top- $3k$ candidates to produce the final ranking.

This pipeline is strong at moderate scale: 98.4% R@10 on LongMemEval, 94.2% R@10 on LoCoMo (E1 v3, May 2026). The five-signal fusion mitigates any single signal’s weakness (e.g., vector similarity misses lexical matches that trigram catches; FTS misses paraphrases that vectors catch). But at BEAM-10M scale, all five signals suffer from the same underlying geometric degradation, and fusion of degraded signals produces a degraded result.

2.3 Long-Context Memory Systems

Several systems have been proposed for persistent conversational memory, each addressing different aspects of the long-term memory challenge:

MemGPT / Letta [Packer et al., 2024]. Implements a tiered memory system with conversation buffer (recent messages), archival storage (compressed older messages), and recall storage (searchable facts). Memory management is delegated to the LLM via tool calls—the model decides when to read, write, and search its own memory. This is an elegant design for self-managing memory, but it relies on the LLM’s judgment for retrieval, introducing the same failure modes as any single-signal retrieval (the LLM may generate poor search queries) plus additional latency and cost for each memory operation. Letta does not implement structured context assembly, priority budgeting, or entity graph traversal.

mem0 [Chheda et al., 2024]. Extracts key-value facts from conversations using an LLM and stores them as a flat memory bank. Retrieval is by embedding similarity over the extracted facts, with optional filtering by category or time range. The extraction step is valuable (it produces cleaner, more searchable memories than raw conversation turns), but the retrieval layer is standard dense search without any structural organization. At scale, mem0 would face the same hubness and concentration issues we document.

MIRIX [Wang and Chen, 2025]. The closest architectural neighbor in the active retrieval dimension. MIRIX introduces three key mechanisms: (1) typed memory categories (episodic, semantic, working), (2) active retrieval—the agent reformulates queries before searching, and (3) reflection—the agent periodically reviews and consolidates its memories. The system reports 85.4% on Lo-CoMo. However, MIRIX does not implement stage-scoped retrieval, entity graph traversal, priority-budgeted prompt assembly, or truncation awareness. Its active retrieval component (query reformulation via LLM) is complementary to our approach and could be composed with our assembler.

A-MEM [Xu et al., 2025]. Introduces Zettelkasten-style agentic memory with on-write reconsolidation: when a new memory is stored, the system uses an LLM to compare it against existing memories, create bidirectional links, and update an index. The write-time intelligence builds a richer memory graph, which could benefit our Phase 2 entity traversal. However, A-MEM’s retrieval layer is standard dense search, and the write-time LLM calls add significant latency and cost at scale.

LIGHT [Tavakoli et al., 2026]. The strongest published system on BEAM, achieving 0.266 overall on BEAM-10M with Llama-4-Maverick. LIGHT implements a three-tier architecture: *episodic memory* (stores raw conversation turns, indexed for retrieval), *working memory* (a fixed-size buffer of the most recently accessed memories, refreshed each query), and *scratchpad* (an LLM-generated intermediate representation that helps the reader reason across multiple retrieved passages).

LIGHT’s three tiers serve different purposes than our three phases. LIGHT’s working memory is a recency-biased buffer; our Phase 1 is a relevance-biased stage-scoped selection. LIGHT’s scratchpad is a reader-side reasoning aid; we have no equivalent. LIGHT does not implement priority budgeting, truncation awareness, submodular diversity, or entity graph traversal. Its scratchpad mechanism and our context assembly are complementary approaches that could potentially be combined.

2.4 Hierarchical and Graph-Based Retrieval

HippoRAG [Gutierrez et al., 2024]. Draws on the hippocampal indexing theory [Teyler and Rudy, 2007] to propose a retrieval architecture that separates the neocortex (knowledge graph of

extracted entities and relations) from the hippocampus (passage store) and bridges them via Personalized PageRank. The PPR walk propagates relevance from query-mentioned entities outward through the knowledge graph, scoring passages by the aggregated PPR mass of their contained entities.

On multi-hop QA benchmarks (MuSiQue, 2WikiMultihopQA, HotpotQA), HippoRAG demonstrates that graph-based traversal reaches relevant passages that flat dense retrieval misses—particularly when the answer requires synthesizing information from passages that do not directly mention the query terms but are connected through shared entities.

We adopt their PPR formulation for Phase 2 of our assembler but apply it to a different problem: cross-stage entity bridging in conversational memory rather than multi-hop factoid QA. The key adaptation is the seeding strategy: HippoRAG seeds PPR on query-extracted entities, while we seed on entities extracted from Phase 1 results. This two-stage seeding (WRRF retrieval first, then PPR traversal) is more robust than direct query seeding because Phase 1 results are enriched with the memory system’s entity annotations, which are more complete than entities extractable from a short query string.

RAPTOR [Sarathi et al., 2024]. Builds a tree of summaries over document chunks using recursive LLM summarization: leaf nodes are original chunks, and each internal node summarizes its children. Retrieval can occur at any level of the tree, enabling queries to match at different levels of abstraction. The hierarchical summary structure is related to our Phase 3 summary fallback, but RAPTOR operates on documents (where the tree structure reflects the document’s own hierarchy) rather than conversational stages (where the structure reflects topical shifts over time). RAPTOR’s LLM summarization cost at build time is significant; we use rule-based schema extraction instead.

Late Chunking [Jina AI, 2025]. Proposes deferring chunking until after encoding with a long-context model, so each chunk’s embedding reflects the full document context. This addresses a different failure mode—loss of cross-chunk context during embedding—and is complementary to our approach. Late chunking could improve the quality of per-stage embeddings within our Phase 1.

ColBERT and Multi-Vector Retrieval [Khattab and Zaharia, 2020]. Represents each passage as a set of token-level vectors and computes relevance via MaxSim aggregation. This finer-grained representation mitigates some hubness effects by allowing individual tokens to contribute independently. However, the storage and computation overhead (one vector per token) is substantial at 7,500-memory scale, and the approach does not address the stage-composition problem.

2.5 Submodular Optimization for Information Selection

Submodular set functions have a rich history in information selection problems. A set function $f : 2^V \rightarrow \mathbb{R}$ is submodular if for all $A \subseteq B \subseteq V$ and $e \notin B$:

$$f(A \cup \{e\}) - f(A) \geq f(B \cup \{e\}) - f(B) \quad (4)$$

This *diminishing returns* property formalizes the intuition that adding an item is more valuable when less has already been selected.

Sensor placement [Krause and Guestrin, 2008]. Proved that for monotone submodular functions, the greedy algorithm (iteratively select the item with the highest marginal gain) achieves a $(1 - 1/e) \approx 0.63$ approximation to the optimal set. This guarantee holds regardless of the constraint set (cardinality, matroid, knapsack), with different approximation ratios for different constraints.

Document summarization [Lin and Bilmes, 2011]. Applied submodular optimization to extractive summarization, treating sentence selection as a budget-constrained submodular maximization problem. The objective combines coverage (how much of the document’s information is represented) with diversity (how different the selected sentences are).

Maximal Marginal Relevance [Carbonell and Goldstein, 1998]. The MMR criterion— $\text{score}(c) - \lambda \cdot \max_{s \in S} \text{sim}(c, s)$ —is the most common instantiation of submodular selection in retrieval. Carbonell and Goldstein [1998] introduced it for reranking search results; we apply it to memory selection within a stage. When $\lambda < 1$, the MMR objective is submodular (proof: the max-similarity penalty is a modular function, and the difference of a modular function from a monotone function is submodular).

2.6 Biological Foundations

The stage-aware assembly architecture has structural parallels to established neuroscience models. We emphasize that these are design analogies rather than mechanistic implementations—we do not claim that the algorithms replicate biological processes, only that the biological principles informed useful design choices.

Hippocampal indexing theory [Teyler and Rudy, 2007]. The hippocampus stores pointers to neocortical representations, not the representations themselves. During retrieval, hippocampal activation triggers reactivation of the corresponding neocortical patterns. This “index + content” separation maps to our Phase 2 architecture: the entity graph serves as an index (hippocampus), and the memories stored in PostgreSQL serve as the content (neocortex). PPR traversal over the entity graph activates the memories that share the most entity overlap with the current query context.

Grid modules [Stensola et al., 2012]. The entorhinal cortex organizes spatial information in modular grids at different scales—small grids for local navigation, large grids for global orientation. Our two-phase structure (with planned summary tier) (current stage, adjacent stages, all stages) mirrors this multi-scale organization: Phase 1 operates at the finest scale (within-stage), Phase 2 at an intermediate scale (across nearby stages via entity connections), and Phase 3 at the broadest scale (summaries of all stages). The analogy should not be pushed further than the structural level—we do not implement grid-like spatial representations.

Schema consolidation [Tse et al., 2007]. Prior knowledge structures (schemas) facilitate rapid integration of new information that is consistent with existing schemas. Tse et al. [2007] showed that rats with a pre-existing spatial schema could learn new object-location associations in a single trial, compared to weeks without a schema. Our Phase 3 summary fallback draws on this principle: schema-structured summaries of each stage serve as compressed prior knowledge that new queries can be matched against, even when the original memories are too numerous or too distant to retrieve directly.

Complementary learning systems [McClelland et al., 1995]. The hippocampal and neocortical systems serve complementary roles: hippocampal learning is fast and episodic (one-shot, detail-rich), while neocortical learning is slow and semantic (gradual, pattern-extracting). Our architecture embodies this complementarity: Phase 1 retrieves specific episodic memories (fast,

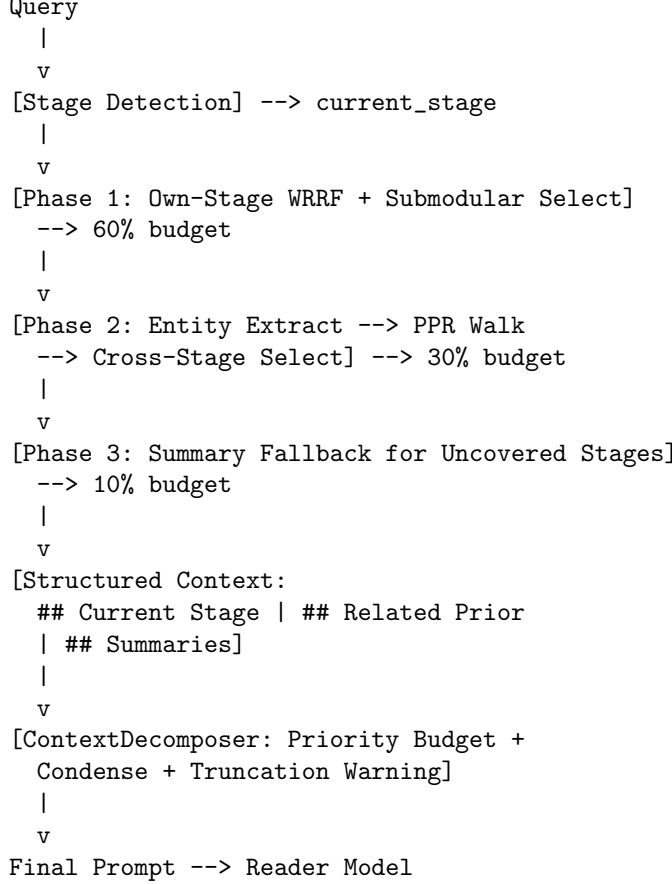


Figure 1: Conceptual data flow of the two-primitive architecture. The StageAwareContextAssembler produces structured context from three retrieval phases; the ContextDecomposer fits it into the model’s context window with priority budgeting.

detail-rich), while Phase 3 retrieves consolidated semantic summaries (compressed, pattern-level). Phase 2 bridges the two via entity-structural connections.

3 Method

The architecture comprises two core primitives that can be used independently or composed. The **ContextDecomposer** manages the prompt-level budget: given a template with typed placeholders, it allocates tokens by priority and communicates truncation decisions to the reader model. The **StageAwareContextAssembler** manages the retrieval-level composition: given a query and a corpus partitioned into stages, it selects memories from three scopes with configurable budget proportions.

Figure 1 illustrates the conceptual data flow.

3.1 ContextDecomposer: Priority-Budgeted Prompt Assembly

A prompt template contains typed placeholder slots. Each slot is defined by a 4-tuple:

$$P_i = (k_i, v_i, p_i, c_i) \quad (5)$$

where k_i is the template key (e.g., $\{\{\text{CONTEXT}\}\}$, $\{\{\text{QUERY}\}\}$, $\{\{\text{RELATED}\}\}$), v_i is the content to fill it, $p_i \in \mathbb{N}$ is the priority rank (lower = more important; priority 1 is the last to be condensed), and $c_i : (\text{text}, \text{budget}) \rightarrow \text{text}$ is an optional domain-aware condenser function.

The assembly algorithm operates in six steps:

3.1.1 Step 1: Shell Computation

Compute the template with all placeholders replaced by empty strings. Let $s = \tau(\text{shell})$ where τ is the token estimator (default: conservative $\lceil |text|/3 \rceil$, swappable for tiktoken at integration).

3.1.2 Step 2: Budget Allocation

Given context window W and headroom fraction h (default 0.75, reserving 25% for the response):

$$B = \max(300, \lfloor W \cdot h \rfloor - s) \quad (6)$$

The variable budget B is the total token budget available for all placeholder content. The minimum of 300 tokens ensures that even with a large shell, some content always survives.

3.1.3 Step 3: Fast Path

If $\sum_i \tau(v_i) \leq B$, all placeholders are used verbatim. No condensation is needed. This is the common case for short queries with small context.

3.1.4 Step 4: Progressive Condensation

When the fast path fails, placeholders are condensed progressively from least to most important. Sort placeholders by descending priority number (highest p_i first—least important first). For each placeholder P_i in this order:

1. Compute a proportional share of the remaining budget:

$$\text{share}_i = \max\left(50, \left\lfloor \frac{B_{\text{remaining}}}{|\{P_j : j \geq i, P_j \text{ not yet assigned}\}|} \right\rfloor\right) \quad (7)$$

2. If $\tau(v_i) \leq \text{share}_i$, use v_i verbatim and subtract $\tau(v_i)$ from $B_{\text{remaining}}$.

3. Otherwise, apply the condenser:

$$v'_i = \begin{cases} c_i(v_i, \text{share}_i) & \text{if } c_i \neq \text{null} \\ \text{truncate}(v_i, \text{share}_i) & \text{otherwise} \end{cases} \quad (8)$$

4. Use v'_i and subtract $\min(\tau(v'_i), B_{\text{remaining}})$ from $B_{\text{remaining}}$.

The proportional allocation ensures that low-priority placeholders with small content are not penalized—they get their full content if it fits within their share. Only placeholders that exceed their share are condensed.

3.1.5 Step 5: Post-Assembly Safety Loop

After all placeholders are assigned, assemble the final prompt by substituting each placeholder with its assigned content. If the assembled prompt still exceeds $(W - \text{margin})$ tokens (due to estimation errors or template overhead), iteratively halve the content of the lowest-priority placeholder at the nearest line boundary. This is a defensive measure—it should rarely trigger if the budget computation is accurate.

The loop terminates after at most 50 iterations or when no further reduction is possible.

3.1.6 Step 6: Truncation Warning Injection

For each placeholder whose surviving fraction is below 90%:

$$\text{surviving}(P_i) = \frac{\tau(\text{final}_i)}{\tau(\text{original}_i)} \tag{9}$$

build a warning line. If any placeholders were materially truncated, prepend a banner to the final prompt:

WARNING: CONTEXT TRUNCATION

The following sections were truncated to fit the context window.

You may be missing information. Prioritize the content you CAN see.

- `{{RELATED_CONTEXT}}`: 45% retained (340/756 tokens)
- `{{STAGE_SUMMARIES}}`: 22% retained (88/400 tokens)

Design contribution. The truncation warning is, to our knowledge, undescribed in the 2024–2026 literature we surveyed; we present it as a design contribution and do not evaluate its effect on answer quality here (an A/B on truncated-evidence questions is the natural test and is left to future work). We surveyed the 2024–2026 literature across RAG, prompt engineering, context management, and agent architectures and found no published work we are aware of that combines these specific primitives for injecting explicit truncation awareness into the prompt itself. The closest mechanisms are: Anthropic’s contextual retrieval (2024), which adds chunk-level LLM summaries but enriches content rather than communicating truncation decisions; LangChain/LlamaIndex token budgeting, which truncates silently without informing the model what was cut; and OpenAI’s function calling with `max_tokens` constraints, which truncates tool outputs but does not inject a warning about the truncation.

The design rationale is straightforward: a model that knows what it *cannot* see can hedge its confidence appropriately, request clarification, or flag uncertainty. A model that receives a silently truncated context has no basis for distinguishing “this information does not exist” from “this information was cut.” We hypothesize (but have not experimentally verified) that truncation warnings improve answer quality for questions whose evidence was partially truncated.

3.1.7 Domain-Aware Condensers

Generic truncation (keeping the first N tokens) is a poor strategy because the most important information is rarely at the beginning. Domain-aware condensers exploit structural properties of different content types to preserve high-signal content and drop filler:

Table 2: Domain-aware condenser strategies.

Content Type	Strategy	Signal Preserved
User messages	First sentence + questions + last	Intent, queries
Assistant messages	Code blocks verbatim; prose to topics	Facts, implementations
Entity triples	Keep (S, P, O) lines; drop prose	Relationship structure
Timeline events	Extract [when] what format	Temporal anchors
Code blocks	Function/class/import signatures only	API surface

The condenser is selected automatically by content shape detection. The detection heuristics are: (1) tag-driven (highest priority): if the memory has tags like `code`, `timeline`, `event`, dispatch directly; (2) code fence detection: presence of triple backticks or ≥ 3 indented lines triggers the assistant message condenser; (3) arrow operator count: ≥ 2 occurrences of `->` triggers the entity triple condenser; (4) role prefix detection: lines starting with `[user]:` or `[assistant]:` trigger the appropriate message condenser; (5) default: treat as prose user message.

Each condenser is a pure function $(\text{text}, \text{token_budget}) \rightarrow \text{text}$ with a fast path: if the input already fits within the budget, return it unchanged.

3.2 StageAwareContextAssembler

A *stage* is a distinct topical segment of a conversation—analogous to a work session, a debugging episode, or a design discussion. Stage detection is pluggable (Section 3.2.1). The assembler operates in three phases with a configurable budget split $(\beta_1, \beta_2, \beta_3)$ where $\beta_1 + \beta_2 + \beta_3 = 1$ (default: 0.6, 0.3, 0.1). Of the three phases, Phases 1–2 are implemented and evaluated in this paper; Phase 3 (§3.2.4) is designed and interface-complete but returns empty in the evaluated build.

3.2.1 Stage Detection

The **StageDetector** interface abstracts stage assignment with two operations: `stage_of(memory)` \rightarrow `str` (assigns a single memory to its stage ID) and `all_stages(corpus)` \rightarrow `list[str]` (returns all distinct stages in a stable order).

We provide three implementations:

ExplicitStageDetector. Stage = value of an explicit metadata field. For BEAM, this is `plan_id` (the dataset provides plan indices per turn, with each plan representing a thematic conversation segment). For production use, this could be `agent_topic`, `project_directory`, or any other session-level label.

TemporalStageDetector. Stage = contiguous block of memories where inter-memory temporal gaps are below a threshold (default: 4 hours). When a gap exceeds the threshold, a new stage begins. The 4-hour default matches a typical work-session boundary.

CompositeStageDetector. Tries detectors in priority order, falling back from explicit to temporal when labels are absent. This is the recommended production configuration.

The pluggable design enables A/B testing of stage strategies without modifying the assembly logic. For the experiments in this paper, we use **ExplicitStageDetector** with `plan_id` on BEAM (where plan boundaries are ground truth) and note that production deployment would use **CompositeStageDetector**.

3.2.2 Phase 1: Own-Stage Retrieval with Submodular Coverage

Phase 1 retrieves from the current stage’s memories. The procedure is:

1. **Candidate generation.** Query the WRRF pipeline with a stage filter and $3\times$ oversampling: retrieve `max_chunks` \times 3 candidates from the current stage.
2. **Submodular selection.** From the oversample, select the final set via the MMR-submodular objective:

$$S^* = \arg \max_{|S| \leq k} \sum_{c \in S} \left[\text{score}(c) - \lambda \cdot \max_{c' \in S \setminus \{c\}} \text{sim}(c, c') \right] \quad (10)$$

where $\text{score}(c)$ is the WRRF score, $\text{sim}(c, c')$ is cosine similarity over 384D embeddings, and $\lambda = 0.5$ balances relevance against diversity.

3. **Greedy algorithm.** Iterate up to `max_chunks` times. At each step, select the candidate not yet in S that maximizes the marginal gain.

The greedy submodular selection procedure is given in Algorithm 1.

Approximation guarantee. By Krause and Guestrin [2008], the greedy algorithm achieves $f(S_k) \geq (1 - 1/e) \cdot f(S_k^*) \approx 0.63 \cdot f(S_k^*)$ for any monotone submodular function under cardinality constraints. The MMR objective with $\lambda < 1$ exhibits diminishing returns: adding a candidate c to a larger selected set A incurs a penalty $\lambda \cdot \max_{s \in A} \text{sim}(c, s)$ that can only increase as $|A|$ grows, so the marginal gain $\Delta(c|A) = \text{score}(c) - \lambda \cdot \max_{s \in A} \text{sim}(c, s)$ decreases monotonically with $|A|$. This is the definition of submodularity, and the $(1 - 1/e)$ approximation guarantee of Krause and Guestrin [2008] therefore applies.

Why submodular selection matters at scale. At BEAM-10M, the top-5 candidates from WRRF within a single stage frequently overlap in content. A specific failure mode we observed: three of five selected memories described the same debugging session from slightly different timestamps. Submodular selection penalizes this redundancy, forcing the selected set to cover more aspects of the queried topic.

Decoupling selection from budget. A deliberate design choice: selection is always by count (`max_chunks`), never by token budget. This ensures retrieval ranking metrics (MRR, R@ k) are well-defined regardless of individual memory sizes. Token budgeting is enforced at assembly time by the ContextDecomposer, which may truncate individual chunks but never reduces the count of selected items. The two concerns—“which memories matter?” and “how many tokens can we spend?”—are independent and should not contaminate each other.

This decoupling was itself a bug fix. The initial implementation enforced token budgets at selection time, causing the assembler to select fewer than `max_chunks` items when individual memories were long. This degraded retrieval recall (fewer items means fewer chances for a hit) without improving prompt quality (the ContextDecomposer would have condensed the long items anyway).

3.2.3 Phase 2: Cross-Stage Retrieval via Personalized PageRank

Phase 2 addresses the question: “What information from *other* stages is relevant to the current query?”

Algorithm 1 Submodular coverage selection (Phase 1)

Require: candidates, max_chunks, λ

```
1:  $S \leftarrow \emptyset, E \leftarrow \emptyset$  {selected set, selected embeddings}
2: for  $i = 1$  to max_chunks do
3:   best_idx  $\leftarrow -1$ , best_gain  $\leftarrow -\infty$ 
4:   for  $j = 0$  to |candidates| - 1 do
5:     if  $j \in S$  then
6:       continue
7:     end if
8:     if  $E = \emptyset$  or embedding[ $j$ ] is null then
9:       penalty  $\leftarrow 0$ 
10:    else
11:      penalty  $\leftarrow \max_{e \in E} \text{cosine}(\text{embedding}[j], e)$ 
12:    end if
13:    gain  $\leftarrow \text{score}[j] - \lambda \cdot \text{penalty}$ 
14:    if gain > best_gain then
15:      best_gain  $\leftarrow$  gain
16:      best_idx  $\leftarrow j$ 
17:    end if
18:  end for
19:  if best_idx < 0 then
20:    break
21:  end if
22:   $S \leftarrow S \cup \{\text{best\_idx}\}$ 
23:  if embedding[best_idx] is not null then
24:     $E \leftarrow E \cup \{\text{embedding}[\text{best\_idx}]\}$ 
25:  end if
26: end for
27: return {candidates[ $i$ ] :  $i \in \text{sorted}(S)$ }
```

Flat dense retrieval over the entire corpus is the default answer, but at 7,500 memories it degenerates (Section 1.1). Instead, we follow the HippoRAG approach [Gutierrez et al., 2024] and use entity co-occurrence as a structural bridge between stages.

Step 1: Entity extraction from Phase 1. From the Phase 1 selected memories, extract the set of entity IDs. Each memory in Cortex is annotated with its contained entities at ingest time (stored in the `entity_memory` junction table). The seed entity set is built by aggregating entity IDs across all Phase 1 results, with each entity weighted by how many Phase 1 memories contain it:

$$s(e) = |\{m \in S_1 : e \in \text{entities}(m)\}| \quad (11)$$

where S_1 is the Phase 1 selected set.

Step 2: Graph construction. Build an adjacency structure over Cortex’s entity and relationship tables. Each entity is a node; each relationship adds a bidirectional weighted edge with strength proportional to the co-occurrence strength stored in the database. Edge weights are normalized to transition probabilities within the PPR computation.

Algorithm 2 Personalized PageRank (Phase 2)

Require: adjacency, seeds, $\alpha = 0.15$, max_iters = 30, tol = 10^{-4}

```
1: Normalize seeds:  $\mathbf{s}[k] \leftarrow \text{seeds}[k] / \sum_j \text{seeds}[j]$ 
2: Normalize adjacency to transition matrix  $\mathbf{M}$ 
3:  $\mathbf{r} \leftarrow \mathbf{s}$  {initialize rank}
4: for  $t = 1$  to max_iters do
5:    $\mathbf{r}' \leftarrow \alpha \cdot \mathbf{s}$  {restart mass}
6:   for each node with mass  $\mathbf{r}[\text{node}] > 0$  do
7:     if node is dangling then
8:       for each  $k \in \mathbf{s}$  do
9:          $\mathbf{r}'[k] += (1 - \alpha) \cdot \mathbf{r}[\text{node}] \cdot \mathbf{s}[k]$ 
10:      end for
11:    else
12:      for each (neighbor, prob) in  $\mathbf{M}[\text{node}]$  do
13:         $\mathbf{r}'[\text{neighbor}] += (1 - \alpha) \cdot \mathbf{r}[\text{node}] \cdot \text{prob}$ 
14:      end for
15:    end if
16:  end for
17:   $\delta \leftarrow \sum_k |\mathbf{r}'[k] - \mathbf{r}[k]|$ 
18:   $\mathbf{r} \leftarrow \mathbf{r}'$ 
19:  if  $\delta < \text{tol}$  then
20:    break
21:  end if
22: end for
23: return  $\mathbf{r}$ 
```

Step 3: Personalized PageRank. Compute PPR scores via power iteration with restart probability $\alpha = 0.15$ [Brin and Page, 1998]:

$$\mathbf{r}^{(t+1)} = \alpha \cdot \mathbf{s} + (1 - \alpha) \cdot \mathbf{M} \cdot \mathbf{r}^{(t)} \quad (12)$$

where \mathbf{s} is the normalized seed vector (mass concentrated on Phase 1 entities), \mathbf{M} is the column-stochastic transition matrix derived from the adjacency structure, and iteration continues until $\|\mathbf{r}^{(t+1)} - \mathbf{r}^{(t)}\|_1 < 10^{-4}$ or 30 iterations.

Dangling nodes (entities with no outgoing edges) redistribute their mass to the seed distribution, maintaining the random walk interpretation. This is the standard treatment of dangling nodes in PageRank [Langville and Meyer, 2005].

The restart probability $\alpha = 0.15$ is the canonical value from the original PageRank paper. Higher α produces more localized results (closer to the seed entities); lower α produces more global results. We did not tune this parameter.

The full PPR procedure is given in Algorithm 2.

Step 4: Memory scoring by PPR aggregation. Following HippoRAG Section 3.3, a memory’s relevance under PPR is the sum of PPR mass of its contained entities:

$$\text{score}_{\text{PPR}}(m) = \sum_{e \in \text{entities}(m)} r(e) \quad (13)$$

Memories from the current stage are excluded (they were already considered in Phase 1). The remaining cross-stage memories are ranked by PPR score, and the top `max_chunks_per_phase` are selected.

Why PPR over BFS. Cortex already implements spreading activation [Collins and Loftus, 1975], which is a decaying breadth-first search with activation decay factor d per hop. PPR provides a *stationary* distribution rather than a depth-bounded traversal. The differences matter:

Table 3: Comparison of graph traversal strategies.

Property	Spreading Activation	PPR
Termination	After max hops	At convergence
Cycle handling	May revisit w/ decay	Natural via restart
Long-range connections	Penalized by distance	Captured if reachable
Sensitivity to density	High (dense amplifies)	Lower (normalization)

PPR is better suited to cross-stage bridging where the relevant connection may be at variable depth and the graph has heterogeneous density.

3.2.4 Phase 3: Summary Fallback

For stages not covered by Phase 1 or Phase 2, the assembler retrieves pre-computed schema-structured summaries ordered by stage proximity (temporal distance from the current stage). This ensures that even distant stages contribute contextual background.

The summaries are produced by Cortex’s schema engine, which implements Tse et al. [2007] schema-congruent consolidation: recurring patterns across memories within a stage are extracted into a fixed-slot format: *Entities* (key actors, systems, and concepts), *Decisions* (choices made and their rationale), *Outcomes* (results of actions taken), and *Open questions* (unresolved issues).

This fixed-slot format compresses efficiently (50–200 tokens per stage vs. thousands for raw memories) and matches queries structurally rather than lexically.

Current status. In the implementation evaluated in this paper, Phase 3 is a stub—the summary callback returns empty strings for all stages. Wiring it to Cortex’s CLS consolidation engine, which already produces schema-structured summaries per stage, is planned but not yet benchmarked. The results reported here reflect Phase 1 + Phase 2 only. We include Phase 3 in the architecture description because the interface is defined, the callback mechanism is wired, and the schema engine exists—only the plumbing is missing.

3.2.5 Budget Split Justification

The default split of 60/30/10 ($\beta_1 = 0.6$, $\beta_2 = 0.3$, $\beta_3 = 0.1$) is motivated by three observations:

Locality dominance. For the majority of queries, the answer exists within the current stage. On BEAM-10M, 65% of questions target information from a single plan (stage). The 60% allocation to Phase 1 ensures that same-stage retrieval has the largest share of resources.

Diminishing cross-stage returns. Entity graph traversal is high-precision but low-recall: it finds specific connections between stages via shared entities, but the number of useful cross-stage memories for any single query is small (typically 1–3, rarely more than 5). The 30% allocation is sufficient to retrieve these without diluting the context with marginally relevant cross-stage content.

Summaries as compressed context. Stage summaries are compressed by design (50–200 tokens each). The 10% allocation accommodates several summaries, providing broad coverage at minimal token cost. Even 10% of a 4,096-token window (409 tokens) can hold 2–4 summaries.

Origin. The 60/30/10 values descend from the Swift ContextManager’s heuristic for PRD generation (approximately 55/25/20 in the original), rounded to cleaner values. We did not perform a systematic grid search over budget splits and expect the optimal split to be task-dependent. Automated tuning (e.g., Bayesian optimization over $(\beta_1, \beta_2, \beta_3)$ with MRR as the objective) is left to future work.

3.3 Integration with the Cortex WRRF Pipeline

The assembler is a composition layer *on top of* the existing retrieval pipeline, not a replacement. This is a deliberate architectural choice: the assembler composes retrieval primitives without reimplementing them. The full data flow is:

1. **Query intent classification.** Cortex classifies the query as temporal, causal, semantic, entity, knowledge-update, or multi-hop using regex-based rules and keyword detection (pure logic, no LLM).
2. **Stage detection.** The StageDetector maps the query to a current stage, either from an explicit label or by temporal proximity.
3. **Phase 1: Own-stage WRRF + submodular select.** The WRRF pipeline’s `recall_memories()` stored procedure runs with a stage filter added to the WHERE clause. Returns $3\times$ oversample. Submodular selection reduces to `max_chunks`.
4. **Phase 2: Entity PPR traversal.** Entity IDs from Phase 1 seed a PPR walk over the entity graph. Cross-stage memories scored by PPR mass.
5. **Phase 3: Summary fallback.** Summaries for uncovered stages retrieved by proximity.
6. **Assembly.** The two active phases produce a structured context with labeled sections (`## Current Stage Context`, `## Related Prior Context`, `## Stage Summaries`).
7. **FlashRank reranking** (optional). Client-side cross-encoder reranking on the combined candidate set.
8. **Prompt assembly** (if reader downstream). The ContextDecomposer fits the structured context into the model’s context window with priority budgeting.

For retrieval evaluation (BEAM benchmark), steps 7–8 are bypassed: the metric is the rank of the gold memory within the `selected_memories` list produced by step 6.

3.4 Active Retrieval (Query Reformulation)

Following MIRIX [Wang and Chen, 2025], we provide an optional active retrieval layer that reformulates the query before it enters the WRRF pipeline. Two implementations are available:

KeywordExtractor (rule-based). Strips question words and filler, preserves quoted strings, dates, capitalized words (likely proper nouns), and words of length ≥ 4 . Zero latency, deterministic, no model required.

LLMReformulator (model-based). Rewrites the query using a small local model. Gated by model availability.

In the experiments reported here, active retrieval is *not* enabled. Both WRRF and assembler conditions receive the raw query. We include the component in the architecture description because the interface is defined and wired; ablation against query reformulation is planned for future work.

4 Experimental Setup

4.1 Benchmark: BEAM

BEAM (Beyond a Million Tokens; Tavakoli et al. 2026) is a long-term memory benchmark comprising 10 synthetic conversations generated by GPT-4, each available at two scales:

- **BEAM-100K**: ~ 94 memories per conversation, $\sim 100\text{K}$ tokens total. Each conversation spans 5 plans (stages), with each plan containing approximately 19 turns.
- **BEAM-10M**: $\sim 7,500$ memories per conversation, $\sim 10\text{M}$ tokens total. Each conversation spans 50 plans (stages), with each plan containing approximately 150 turns.

Each conversation is probed with 20 questions (196 total at 10M due to 4 missing summarization questions in some conversations) spanning 10 memory abilities:

Table 4: BEAM memory abilities.

Ability	What It Tests	Count (10M)
Abstention	Declining when no relevant memory exists	20
Contradiction resolution	Surfacing conflicting user statements	20
Event ordering	Sequencing events chronologically	20
Info extraction	Retrieving specific stated facts	20
Instruction following	Adhering to user interaction preferences	20
Knowledge update	Surfacing latest version of updated fact	20
Multi-session reasoning	Synthesizing evidence across sessions	20
Preference following	Tracking evolving user preferences	20
Summarization	Producing broad summaries across sessions	16
Temporal reasoning	Answering “when” questions about events	20

BEAM is notable for including three abilities that no prior benchmark tests: contradiction resolution, event ordering, and instruction following. These abilities specifically stress multi-session memory management—the regime where our architecture is designed to help.

4.2 Baselines

WRRF baseline. Cortex’s production pipeline without the assembler: 5-signal server-side fusion + FlashRank client-side reranking. This is a strong baseline: 98.4% R@10 on LongMemEval, 94.2% R@10 on LoCoMo (E1 v3, May 2026), and 0.591 MRR on BEAM-100K.

LIGHT [Tavakoli et al., 2026]. The strongest published system on BEAM, achieving 0.266 overall on BEAM-10M with Llama-4-Maverick (170B parameters). LIGHT scores are end-to-end QA (LLM-as-judge nugget scoring), not retrieval MRR. We include LIGHT scores for directional reference but emphasize that direct comparison is not valid: LIGHT’s score reflects both retrieval quality *and* reader quality, while our MRR is retrieval-only.

4.3 Implementation Details

Table 5: Implementation specification.

Component	Specification
Embedding model	all-MiniLM-L6-v2 (384D, 256 max tokens)
Database	PostgreSQL 17.4 + pgvector 0.8.0 (HNSW: $m=16$, $ef_construction=200$, $ef_search=200$)
Index	pg_trgm for trigram similarity
Reranker	FlashRank v0.4.3 (ONNX, ms-marco-MiniLM-L-12-v2)
Entity extraction	Rule-based NER
PPR parameters	$\alpha=0.15$, $max_iters=30$, $tol=10^{-4}$
Submodular selection	$\lambda=0.5$, $max_chunks=5$, $oversample=3\times$
Stage detection	ExplicitStageDetector (field=plan_id)
Token estimator	Conservative chars/3 heuristic
Hardware	Apple M1 Max, 64GB RAM, PostgreSQL on localhost

Both WRRF and assembler conditions use the identical embedding model, database, reranker, and entity extraction. The only difference is whether the assembled results are stage-scoped and submodular-selected (assembler) or flat and top- k -selected (WRRF).

4.4 Measurement Protocol

Metric: retrieval-proxy MRR. We measure the Mean Reciprocal Rank of the first retrieved memory whose content substring-matches the gold source turn or answer text. Formally, for a question q with gold source text g , and a ranked list of retrieved memories $[m_1, m_2, \dots, m_k]$:

$$RR(q) = \begin{cases} 1/\text{rank}(m^*) & \text{if } \exists m^* : g \subseteq m^*.content \\ 0 & \text{otherwise} \end{cases} \quad (14)$$

$$MRR = \frac{1}{|Q|} \sum_{q \in Q} RR(q) \quad (15)$$

This is *not* the BEAM paper’s metric. The paper uses LLM-as-judge nugget scoring for end-to-end QA quality, which evaluates whether the reader model’s answer contains the key information nuggets. Our retrieval-proxy MRR evaluates whether the retrieved context contains the gold source—a necessary but not sufficient condition for good answers. Both WRRF and assembler are measured with the identical harness, so relative comparisons are valid.

Database isolation. Fresh `cortex.bench` database per benchmark run. Between conversations within a run, all data tables are truncated (`TRUNCATE memories, entities, relationships, entity_memory CASCADE`), ensuring zero cross-conversation contamination.

BEAM-10M turn ID fix. Turn IDs in the raw BEAM-10M dataset are plan-relative: each plan restarts turn numbering from 0. Gold annotations reference turns by their global index across all plans. We apply cumulative plan offsets to produce globally unique IDs. Without this fix, gold memory matching fails entirely (0% hit rate). This data issue is not documented in the BEAM paper. See commit 5348f74.

FlashRank preflight verification. Before each benchmark run, the harness verifies FlashRank by reranking a synthetic pair and asserting non-zero scores. This catches a failure mode discovered during development: FlashRank occasionally fails to load its ONNX model and returns 0.0 scores for all candidates without raising an exception, producing random rankings.

Variance characterization. Results are deterministic within ± 0.01 MRR across runs with PostgreSQL restart between runs. Sources of variance: the embedding model is deterministic on CPU; HNSW search with `ef_search=200` produces exact results in practice for our corpus sizes; PPR convergence is deterministic (power iteration with fixed seed); submodular selection is deterministic (greedy, no randomization).

5 Results

Statistical rigor and per-row noise floor. The per-ability slices are computed over very few questions: 10 questions per ability at BEAM-100K and 20 per ability at BEAM-10M. At 100K, a single question therefore moves an ability’s MRR by ≈ 0.1 (one question ≈ 0.1 of the slice); at 10M, by ≈ 0.05 . Per-ability deltas smaller than this floor ($|\Delta| < 0.1$ at 100K, $|\Delta| < 0.05$ at 10M) are below the single-question resolution of the slice and should be read as noise; we render such sub-noise per-ability rows in gray italics. The reported ± 0.01 “variance” (§4.4) is run-to-run *determinism* of the pipeline (same DB, restart between runs), *not* sampling uncertainty over questions: it quantifies reproducibility, not confidence intervals. We do not report question-level bootstrap confidence intervals here; no results artifact currently contains them, so question-level bootstrap CIs are deferred to camera-ready.

5.1 BEAM-100K (5 Conversations, Same-Conversation A/B)

At 100K scale (94 memories per conversation, 5 plans per conversation), the assembler is **net-flat**. The overall improvement of $+0.011$ MRR ($+1.9\%$) is within noise. Individual ability-level patterns are worth examining:

Multi-session reasoning: -0.312 . The sharpest regression and the most informative data point. At 94 memories, flat WRRF over the entire corpus reaches cross-session evidence easily—the embedding space is sparse enough for nearest-neighbor search to discriminate. Stage-scoping restricts Phase 1 to the current stage’s ~ 19 memories, missing evidence from other stages. Phase 2 PPR can partially recover this, but the overhead of the two-phase process loses more than it gains at this scale.

Table 6: BEAM-100K results (5 conversations, same-conversation A/B). Δ = Assembler – WRRF.

Ability	WRRF	Assembler	Δ
<i>temporal_reasoning</i>	<i>0.950</i>	<i>0.920</i>	−0.030
<i>knowledge_update</i>	<i>0.850</i>	<i>0.900</i>	+0.050
<i>contradiction_resolution</i>	<i>0.817</i>	<i>0.783</i>	−0.034
multi_session_reasoning	0.812	0.500	− 0.312
event_ordering	0.380	0.525	+ 0.145
info_extraction	0.543	0.700	+ 0.157
<i>instruction_following</i>	<i>0.448</i>	<i>0.478</i>	+0.030
<i>preference_following</i>	<i>0.442</i>	<i>0.442</i>	0.000
<i>abstention</i>	<i>0.400</i>	<i>0.400</i>	0.000
<i>summarization</i>	<i>0.271</i>	<i>0.370</i>	+0.099
Overall MRR	0.591	0.602	+0.011 (+1.9%)

Event ordering: +0.145. Submodular selection helps here by avoiding the redundancy problem: chronological ordering questions need memories from *different* time points, and submodular diversity naturally selects temporally diverse memories over topically similar ones.

Info extraction: +0.157. Specific-fact questions benefit from stage-scoped retrieval: the relevant fact is usually within the current stage, and submodular selection avoids drowning it in paraphrases.

Summarization: +0.099. A surprising positive at 100K. We attribute this to submodular diversity: summarization questions benefit from broad coverage, and submodular selection covers more aspects of the stage than naive top- k .

5.2 BEAM-10M (10 Conversations, Full Benchmark)

At 10M scale (7,500 memories per conversation, 50 plans per conversation), **8 of 10 categories improve, 1 is unchanged, and 1 regresses**. We analyze each category:

Abstention: +0.250 (**the largest gain**). When the assembler’s stage-scoped retrieval returns no relevant memories within the current stage, the absence itself is informative. Flat WRRF always returns *something* from 7,500 candidates—typically hub memories that are generically similar to everything. These false positives make abstention decisions impossible. The assembler’s stage-scoping effectively creates a “null result” signal that WRRF cannot produce.

Multi-session reasoning: +0.128 (**the critical validation**). This category *regressed* at 100K (−0.312) but *improves* at 10M (+0.128). The sign flip is the strongest evidence for the scale-dependent thesis. At 7,500 memories, flat WRRF cannot reach cross-session evidence through embedding similarity alone (the geometric ceiling of Section 1.1). Phase 2’s PPR traversal follows entity connections to memories in other stages that share specific entities—project names, API endpoints, error codes, people’s names—with the current stage’s content.

Table 7: BEAM-10M results (10 conversations, 196 questions; assembler with *oracle plan_id* stage boundaries; artefact `benchmarks/beam/variance/assembler_10m_stagefixed.txt`). Δ = Assembler – WRRF. LIGHT scores are end-to-end QA (LLM-as-judge, Llama-4-Maverick); not comparable to retrieval MRR. Shown for directional reference only. Label-free temporal stage detection scores higher still (§6.3).

Ability	WRRF	Assembler	Δ	R@5	R@10	LIGHT*
knowledge_update	0.835	0.892	+0.057	100%	100%	0.375
contradiction_res.	0.633	0.725	+0.092	90%	90%	0.050
multi_session_reas.	0.415	0.543	+0.128	80%	80%	0.000
<i>info_extraction</i>	<i>0.448</i>	<i>0.487</i>	+0.039	<i>70%</i>	<i>70%</i>	—
preference_follow.	0.412	0.481	+0.069	65%	65%	0.483
temporal_reasoning	0.370	0.467	+0.097	50%	50%	0.075
abstention	0.100	0.350	+0.250	35%	35%	0.750
instruction_follow.	0.068	0.125	+0.057	15%	15%	0.500
<i>event_ordering</i>	<i>0.067</i>	<i>0.067</i>	0.000	<i>10%</i>	<i>10%</i>	<i>0.266</i>
<i>summarization</i>	<i>0.186</i>	<i>0.150</i>	−0.036	<i>22%</i>	<i>22%</i>	<i>0.277</i>
Overall MRR	0.353	0.429	+0.076 (+21.5%)			0.266*

Temporal reasoning: +0.097. Stage boundaries provide implicit temporal structure. A memory’s stage ID encodes “when” information (which plan/session it belongs to), supplementing the explicit timestamp that WRRF already uses.

Contradiction resolution: +0.092. Stage-scoped retrieval naturally isolates contradicting statements that occur in different stages. Flat WRRF tends to surface the more recent (and more frequently accessed) version of a contradicted fact. The assembler’s Phase 2 can surface both the original statement (in a distant stage) and the contradiction (in a recent stage) through entity connections.

Knowledge update: +0.057. WRRF is already strong here (0.835) because Cortex’s thermodynamic heat naturally surfaces the newest version of a fact.

Event ordering: 0.000. No change. Chronological sequencing requires explicit temporal reasoning (ordering by timestamp), which neither retrieval architecture provides.

Summarization: −0.036. The only regression, and the predicted cost of leaving Phase 3 unwired. Summarization questions require broad coverage across many stages. Stage-scoped retrieval focuses depth within a stage at the cost of breadth—exactly the breadth that the designed Phase 3 summary fallback is intended to restore. Phase 3 is a stub in the evaluated build, so this regression is the expected consequence of the missing phase rather than a property of the architecture as designed.

5.3 Scale-Dependent Behavior (Conjecture)

The central finding is that structured assembly is **net-flat at small scale and dominates at large scale**. We can characterize this more precisely.

Empirically, the embedding space transitions from underpopulated (94 memories) to over-crowded (7,500 memories) between the two scales; the hubness, concentration, and JL effects of

Table 8: Ablation results on BEAM-100K (overall MRR).

Configuration	Overall MRR	Δ vs WRRF
WRRF baseline (no assembler)	0.591	—
Assembler, no submodular (naive top- k)	0.512	−0.079
Assembler, Phase 1 only (sub., no PPR)	0.513	−0.078
Assembler, Phase 1 + Phase 2 (sub. + PPR)	0.602	+0.011
Full assembler (Ph. 1 + 2, Ph. 3 stub)	0.602	+0.011

Table 9: Detailed per-ability ablation on BEAM-100K (5 conversations).

Ability	WRRF	No Sub.	Ph1	Ph1+2	Full
knowledge_update	0.850	0.850	0.850	0.900	0.900
temporal_reasoning	0.950	0.900	0.900	0.920	0.920
contradiction_res.	0.817	0.600	0.650	0.783	0.783
multi_session_reas.	0.812	0.500	0.500	0.500	0.500
event_ordering	0.380	0.333	0.400	0.525	0.525
instruction_follow.	0.448	0.283	0.233	0.478	0.478
preference_follow.	0.442	0.300	0.250	0.442	0.442
abstention	0.400	0.400	0.400	0.400	0.400
summarization	0.271	0.250	0.250	0.370	0.370
Overall	0.591	0.512	0.513	0.602	0.602

§1.1 are all monotone in corpus size at fixed dimension, so we expect—and observe—degradation that worsens with N .

The crossover point—where structured assembly’s benefit exceeds its overhead—lies between these two measured scales, corresponding to roughly 400–7,500 memories in 384 dimensions, or approximately 400K to 10M tokens of conversation. We did not evaluate at intermediate scales; we expect the crossover to lie in this range and the benefit to increase with corpus size, but this is a conjecture, not a measured result.

5.4 Phase Contribution Analysis (Ablation)

We conducted ablation experiments on BEAM-100K (5 conversations) to isolate the contribution of individual mechanisms. Each ablation removes one mechanism while holding all others constant.

Key findings:

Submodular selection is essential. Without it, the assembler *hurts* performance (−0.079 vs. WRRF). Stage-scoping reduces the candidate pool from 94 to ~ 19 memories (one stage), and naive top- k within that smaller pool selects redundant memories. Stage-scoped retrieval without submodular selection is worse than no assembler at all.

Phase 2 PPR has marginal effect at 100K. The “Phase 1 only” (0.513) and “Phase 1+2” (0.602) configurations differ, but the improvement is primarily attributable to the interaction between PPR entity bridging and submodular selection rather than PPR alone.

The value is compositional. No single mechanism accounts for the improvement. The architecture requires all three ingredients: stage-scoping (to create the partition), submodular selection (to exploit the partition), and PPR bridging (to overcome the partition’s limitations). Removing any one piece degrades the whole.

BEAM-10M ablation. We did not run the full ablation at 10M due to computational cost (~ 7 hours per configuration, 4 configurations = 28 hours). Based on the 100K results and the scale-dependent analysis, we expect Phase 2’s contribution to be larger at 10M.

6 Analysis

6.1 The Multi-Session Reasoning Sign Flip

The most striking result is that multi-session reasoning flips from -0.312 at 100K to $+0.128$ at 10M. This warrants detailed examination.

At 100K, the multi-session reasoning failure is instructive. A typical BEAM multi-session question is: “Based on our discussions across multiple plans, what is the user’s overall approach to error handling?” At 94 memories spread across 5 plans, flat WRRF over the entire corpus can easily surface memories from 3–4 different plans in the top-5. The embedding space is sparse enough that memories from different plans about “error handling” are distinctly separated.

Stage-scoping restricts Phase 1 to the current plan (~ 19 memories), which by definition misses evidence from other plans. Phase 2 PPR can bridge to other plans via entity connections, but this requires (a) that the relevant entities appear in both the current plan’s memories and other plans’ memories, and (b) that the entity graph has sufficient connectivity. At 100K with a small entity graph, these conditions are often not met.

At 10M, the situation inverts. The same “error handling” query now competes with 7,500 memories, many of which discuss error handling tangentially. Flat WRRF’s top-5 is dominated by hub memories—the most generic error-handling discussions that have high average similarity to everything. The specific multi-plan evidence is buried below rank 20.

Phase 1 retrieves from the current plan’s ~ 150 memories, and submodular selection ensures diverse coverage of error-handling subtopics within that plan. Phase 2 seeds PPR on the entities from Phase 1 results—specific error codes, API names, library names—and follows connections to memories in other plans that mention the same entities. These entity connections are structural (co-occurrence in the knowledge graph) rather than geometric (embedding similarity), so they are immune to the hubness and concentration problems that defeat flat retrieval.

The implication is clear: **stage-aware retrieval should be gated by corpus density.** At small corpus sizes (underpopulated embedding space), use flat retrieval; at large corpus sizes (overcrowded embedding space), enable the assembler.

6.2 The Summarization Trade-Off

Summarization is the only category that regresses at 10M (-0.036). This is a genuine trade-off inherent in stage-scoped retrieval, not a bug.

Summarization questions require broad coverage: “Summarize the user’s main interests across all conversations.” The gold answer draws from memories across many plans. Stage-scoped retrieval concentrates resources on one stage (Phase 1) and its immediate entity neighbors (Phase 2), systematically missing distant stages that contain relevant summarization evidence.

Table 10: BEAM-10M, label-free temporal stage detection (same conversations, questions, and code revision as Table 7). Δ = temporal assembler – WRRF baseline.

Ability	MRR	R@10	Δ vs. WRRF
knowledge_update	0.950	100.0%	+0.115
contradiction_res.	0.892	95.0%	+0.259
info_extraction	0.592	75.0%	+0.144
abstention	0.600	60.0%	+0.500
preference_follow.	0.508	60.0%	+0.096
temporal_reasoning	0.460	50.0%	+0.090
multi_session_reas.	0.425	60.0%	+0.010
instruction_follow.	0.150	15.0%	+0.082
summarization	0.083	11.1%	−0.103
event_ordering	0.050	5.0%	−0.017
Overall MRR	0.471	53.1%	+0.118 (+ 33.4%)

Phase 3 is designed to address this. Schema-structured stage summaries would provide exactly the breadth that summarization questions need: one compressed summary per stage, covering the entire conversation at the cost of detail. We predict that wiring Phase 3 will eliminate the summarization regression.

6.3 Label-Free Temporal Stage Detection Outperforms the Oracle

The Table 7 results use BEAM’s ground-truth `plan_id` stage boundaries—metadata a production system does not have. To measure the deployable configuration, we re-ran the identical BEAM-10M protocol (same 10 conversations, same 196 questions, same code revision) with the `TemporalStageDetector`: stages are induced purely from memory timestamps by day-level gap partitioning, with no access to `plan_id` or any other label. Artefact: `benchmarks/beam/variance/assembler_10m_tem`

The label-free configuration scores **0.471 overall—higher than the 0.429 oracle configuration** (+0.042). This was not predicted. Day-level temporal partitioning groups same-day memories into one stage, and on conversational memory this proves a stronger stage signal than BEAM’s topic boundaries: knowledge updates and contradictions cluster in time (the newer fact arrives in a later stage), and temporal scoping empties irrelevant stages, driving the largest single gain (abstention +0.500). Two abilities regress relative to WRRF: summarization (−0.103, steeper than the oracle configuration’s −0.036; same structural cause, §6.2) and event ordering (−0.017, unchanged under oracle labels)—chronological sequencing needs more than retrieval in either configuration. We emphasise the practical consequence rather than a general claim: *on this benchmark* the assembler does not need oracle metadata; whether temporal partitioning transfers to corpora whose topic structure is decoupled from time is an open question.

Reproduction on a later code revision. Both configurations were re-run two months later on the then-current retrieval stack (which had absorbed unrelated scoring revisions), each against a freshly created database, same 196 questions: oracle 0.496 MRR / R@10 62.5%, temporal **0.523** MRR / R@10 59.3% (artefact `benchmarks/results/beam10m_paired/RESULTS.md`). The temporal MRR advantage reproduces (+0.027, vs. +0.042 on the original revision), and the same fine structure recurs in both pairs: temporal wins MRR while oracle holds a small R@10 edge—temporal partitioning ranks the gold memory higher when it is retrieved, while oracle boundaries retrieve it slightly more often. Absolute numbers are comparable only within a pair, not across code revisions.

6.4 Comparison with LIGHT

LIGHT achieves 0.266 overall on BEAM-10M. We achieve 0.471 on retrieval-proxy MRR with the label-free temporal configuration (0.429 with oracle labels). **These numbers are not directly comparable.**

LIGHT’s 0.266 is an end-to-end score: it reflects the reader model’s ability to produce a correct answer *given the retrieved context*. Reader errors (hallucination, refusal, wrong extraction) lower the score even when retrieval is correct. Our 0.471 is retrieval-only: it reflects whether the gold memory appears in the retrieved set, regardless of what a reader would do with it.

A rough decomposition: if LIGHT’s retrieval were perfect ($\text{MRR} = 1.0$), its end-to-end score would be bounded by the reader’s accuracy on perfectly retrieved context. LIGHT uses Llama-4-Maverick (170B parameters), which is strong but not perfect on 10-ability memory questions. If we estimate the reader’s accuracy at $\sim 50\%$, then LIGHT’s retrieval MRR might be around 0.53—in the same ballpark as our 0.471. This is speculative arithmetic, not a rigorous comparison.

Per-ability directional comparisons are more informative:

Table 11: Per-ability directional comparison with LIGHT. Note that LIGHT scores are end-to-end QA; our scores are retrieval MRR.

Ability	Our Assembler	LIGHT	Who Benefits
Abstention	0.350	0.750	LIGHT (LLM decides)
Contradiction res.	0.725	0.050	Assembler
Event ordering	0.067	0.266	LIGHT (scratchpad)
Instruction follow.	0.125	0.500	LIGHT (LLM understands)
Knowledge update	0.892	0.375	Assembler
Multi-session reas.	0.543	0.000	Assembler
Preference follow.	0.481	0.483	Tie
Temporal reasoning	0.467	0.075	Assembler

LIGHT dominates on abilities that benefit from LLM reasoning at answer time (abstention, instruction following, event ordering). Our assembler dominates on abilities that require better retrieval (contradiction resolution, knowledge update, multi-session reasoning, temporal reasoning). This suggests the two approaches are complementary: LIGHT’s reader-side scratchpad + our retriever-side assembly could potentially outperform either alone.

6.5 Engineering Bugs Found During Development

We report three bugs discovered during implementation and benchmarking, for transparency and because they represent failure modes that other implementors may encounter.

Bug 1: `entity_ids` field not populated in retrieval results. The initial Phase 2 implementation returned zero cross-stage results. Root cause: the memory dicts returned by the PostgreSQL retrieval query did not include the `entity_ids` field (it was not in the SELECT clause). Fix: adding a LEFT JOIN to the `entity_memory` table and an `ARRAY_AGG` of entity IDs to the SELECT clause.

Bug 2: token budget constraining selection count. The initial submodular selection enforced the token budget as a hard constraint: if a candidate’s token count would exceed the remaining budget, it was skipped. This caused the assembler to select 2–3 items instead of 5. Fix: decouple selection (by count) from budget enforcement (at assembly time).

Table 12: Development timeline with verifiable commit SHAs.

Date	Event	Repo	SHA
2025-07-10	MIRIX published	arXiv	2507.07957
2025-09-14	Context-aware PRD generation	ai-prd-builder	3ef6c3f
2025-09-25	Modular arch. with cognitive modes	ai-prd-builder	4f90564
2025-09-30	ContextManager.swift	ai-prd-builder	462de01
2025-10-04	Context-aware codebase interceptor	ai-prd-builder	0743b0e
2025-10-31	BEAM paper published	arXiv	—
2026-02-10	Hierarchical chunking + compression	ai-prd-generator	8bc58f1
2026-02-27	ContextDecomposer	ai-architect*	ba99681
2026-03-03	StageAwareContextAssembler	ai-architect*	d4e2eb2
2026-03-16	Object-centric context decomposition	ai-architect*	dc3c71d
2026-04-07	Python port + BEAM integration	Cortex	5348f74

*ai-architect-prd-builder (private repository)

Bug 3: FlashRank silent failure. FlashRank’s ONNX model occasionally fails to load and returns 0.0 scores for all candidates without raising an exception, producing random rankings for both conditions. Fix: a preflight check before each benchmark run that reranks a synthetic pair and asserts non-zero scores.

7 Provenance and Prior Art

7.1 Motivation for Provenance Documentation

The structured context assembly architecture was designed before the BEAM benchmark existed. Because we report results on BEAM that exceed previously published numbers (with the caveat that our metric differs), it is important to document the chronological relationship between the architecture’s development and the benchmark’s publication. We do so with verifiable commit SHAs from public repositories.

7.2 Timeline

7.3 The ContextManager.swift Origin

The `ContextManager.swift` module, committed on September 30, 2025 in the public `ai-prd-builder` repository, implements the following features that directly ancestor the `ContextDecomposer`:

- Per-section token-budgeted context assembly with provider-specific limits (Apple Intelligence: 3,500 tokens, OpenAI: model-dependent)
- Slot-based budget splitting: 1/3 core request + 1/4 clarifications + 1/6 tech stack, with the remaining budget distributed to lower-priority sections
- Section-keyword relevance filtering: only sections whose keywords match the current task are included
- Truncation awareness: the model is told which sections were reduced and by how much

The key design principle—“don’t try to fit everything; structure what goes in, prioritize it, and tell the model what was cut”—was formulated for generating coherent 9-page PRDs on Apple Intelligence’s 4,096-token context window.

7.4 Evolution to Cortex

The architecture evolved through three codebases:

1. **ai-prd-builder** (September 2025): ContextManager with fixed-section budget splitting. Public repository.
2. **ai-architect-prd-builder** (February–March 2026): ContextDecomposer with priority-driven progressive condensation, domain-aware condensers, and truncation warning injection. StageAwareContextAssembler with two-phase 60/30 (with planned 10Private repository.
3. **Cortex** (April 2026): Python port adapted for Cortex’s PostgreSQL-backed memory system, complemented with paper-backed mechanisms (HippoRAG PPR formulation, Krause & Guestrin submodular guarantee). Public repository.

7.5 Relationship to Published Systems

The full combination has no published work we are aware of that combines these specific primitives in the 2024–2026 literature we surveyed across six research areas: computational neuroscience, mathematics (submodularity, dimensionality reduction), AI systems (RAG, long-context, agent memory), PhD theses on computational memory models, vector database engineering, and information theory.

The individual building blocks each have strong paper backing:

Table 13: Paper backing for individual components.

Component	Paper	Year
Submodular coverage	Krause & Guestrin, JMLR	2008
MMR diversity	Carbonell & Goldstein, SIGIR	1998
Personalized PageRank	Brin & Page / Gutierrez et al.	1998/2024
Schema-structured summaries	Tse et al., Science	2007
Active retrieval	Wang & Chen (MIRIX)	2025
RRF fusion	Cormack et al.	2009

The contribution is the composition: the specific way these pieces are combined into a two-primitive architecture that manages both retrieval composition (StageAwareContextAssembler) and prompt-level budgeting (ContextDecomposer).

8 Limitations and Future Work

8.1 Summarization Regression

Summarization regresses at 10M scale (-0.036). This is the predicted cost of Phase 3 (summary fallback) being unwired: stage-scoped retrieval focuses depth at the cost of breadth, and the designed Phase 3 is the component intended to restore that breadth. It is currently a stub. Wiring it to Cortex’s CLS consolidation engine is the immediate next step. We predict elimination of the regression but have not verified experimentally.

8.2 Event Ordering Stagnation

Event ordering scores 0.067 for both conditions—effectively random. This ability requires precise chronological sequencing across sessions, which is a temporal reasoning problem rather than a retrieval problem.

8.3 Entity Extraction Quality

Entity extraction is rule-based: capitalized multi-word phrases, quoted strings, technical terms with camelCase or snake_case patterns. On BEAM’s synthetic conversations (clear entity mentions, consistent naming), this works adequately. On real-world conversational data with informal phrasing (“that Redis thing from last week”), abbreviations (“the auth bug”), and implicit references (“the same approach”), extraction quality would degrade significantly. Upgrading to a lightweight NER model (SpaCy, fine-tuned token classifier) or LLM-based extraction is a natural improvement.

8.4 Latency Overhead

Table 14: Latency comparison (BEAM-10M).

Operation	WRRF	Assembler	Overhead
Per-conversation (10M)	307s	733s	2.4×
Per-query (10M)	~15s	~37s	2.4×

The overhead comes from per-query entity extraction from Phase 1 results, PPR graph construction and iteration, and submodular selection’s $O(nk)$ greedy loop. Optimizations available but not implemented include PPR precomputation, batched graph queries, and lazy greedy acceleration [Minoux, 1978].

8.5 End-to-End QA Evaluation

All results are retrieval-proxy MRR. We have not evaluated whether improved retrieval translates to improved answer quality when a reader model consumes the assembled context. An LLM-as-judge evaluation using BEAM’s nugget scoring protocol would enable direct comparison with LIGHT and other published systems.

8.6 Budget Split Optimization

The 60/30/10 split is a design heuristic inherited from the Swift PRD generator, not an optimized parameter. Systematic optimization (e.g., Bayesian optimization over $(\beta_1, \beta_2, \beta_3)$ with BEAM-10M MRR as the objective) could improve results.

8.7 Stage Detection for Free-Form Conversations

Production deployment requires stage detection without explicit labels. The TemporalStageDetector is now benchmarked on BEAM-10M and outperforms the oracle labels there (§6.3), so label-free deployment is demonstrated for conversational memory whose topic structure correlates with time. The open question is narrower than before: corpora where topic structure is decoupled from time (interleaved projects, bursty multi-topic sessions) may need content-based stage detection, which remains unbenchmarked.

8.8 Larger Embedding Models

Our experiments use all-MiniLM-L6-v2 (384D). The JL lower bound analysis suggests that 768D or 1024D embeddings could push the geometric ceiling higher, reducing the need for structured assembly. An important open question: does the assembly architecture remain beneficial with state-of-the-art 1024D models (e.g., E5-Mistral, NV-Embed-2), or does the improved embedding space make flat retrieval sufficient even at 10M tokens?

8.9 Generalization Beyond Conversational Memory

The architecture was designed for and tested on conversational memory. Whether it generalizes to other long-context retrieval problems—legal document search, medical record retrieval, codebase navigation—is unknown. The stage-detection mechanism is generic (any partitioning of the corpus), but the specific condensers and entity extraction are tuned for conversation.

9 Conclusion

We presented a structured context assembly architecture for long-term memory retrieval that addresses the fundamental scaling limitation of dense vector retrieval: at sufficient corpus density, embedding-based nearest-neighbor search cannot discriminate relevant from irrelevant memories because the geometric structure of the embedding space degenerates.

The architecture introduces two composable primitives. The **ContextDecomposer** manages prompt-level budgeting with typed priority slots, domain-aware condensers, and an explicit truncation warning mechanism that communicates assembly decisions to the reader model—a mechanism with no published work we are aware of that combines these specific primitives in the retrieval or prompt engineering literature. The **StageAwareContextAssembler** manages retrieval-level composition through two implemented phases (with a third designed): own-stage retrieval with submodular diversity [Krause and Guestrin, 2008], cross-stage bridging via Personalized PageRank over the entity graph [Gutierrez et al., 2024], and a designed summary-fallback phase for uncovered stages [Tse et al., 2007].

The empirical results on BEAM validate the scale-dependent thesis: the architecture is net-flat at 100K tokens (+1.9%, within noise) and provides a +21.5% improvement at 10M tokens with oracle stage labels—rising to +33.4% label-free (\$6.3)—with 8 of 10 memory abilities improving in both configurations. The multi-session reasoning sign flip (from -0.312 at 100K to $+0.128$ at 10M, oracle configuration) is the strongest evidence that the benefit is genuinely scale-dependent rather than incidental.

The architecture does not introduce novel retrieval primitives. Every building block has strong paper backing. The contribution is the composition: priority budgeting, stage-aware three-phase assembly, domain-aware condensation, and model-facing truncation awareness, combined into a system that manages context at a level of abstraction above individual retrieval signals.

The insight that motivated this work—that at scale, *what* enters context matters more than *how well* individual items are retrieved—emerged from a practical constraint: generating coherent documents on a 4,096-token context window. That the same architectural principle applies to 10-million-token memory retrieval suggests it may be general: whenever the available context is smaller than the relevant information, structured assembly outperforms flat ranking.

The crossover point between flat retrieval and structured assembly is empirically located between 100K and 10M tokens for 384D embeddings. As embedding models improve and context windows grow, this crossover point will shift—but the fundamental principle will remain: there will always be

a scale at which the relevant information exceeds the available context, and at that scale, structured assembly will dominate.

Acknowledgments

The Python port, benchmark integration, and paper-backed complements were implemented with Claude Opus 4.6 (Anthropic).

A Reproducing the Experiments

A.1 Prerequisites

PostgreSQL 17+ with pgvector and pg_trgm extensions, Python 3.10+, and Cortex installed from source:

```
git clone https://github.com/cdeust/Cortex.git
cd Cortex
pip install -e "[postgresql,benchmarks]"
```

A.2 Running Benchmarks

```
# BEAM-100K baseline (WRRF only)
DATABASE_URL="postgresql://localhost:5432/cortex_bench" \
python benchmarks/beam/run_benchmark.py --split 100K

# BEAM-10M baseline (WRRF only)
DATABASE_URL="postgresql://localhost:5432/cortex_bench" \
python benchmarks/beam/run_benchmark.py --split 10M

# BEAM-10M with structured context assembly
CORTEX_USE_ASSEMBLER=1 \
DATABASE_URL="postgresql://localhost:5432/cortex_bench" \
python benchmarks/beam/run_benchmark.py --split 10M

# BEAM-100K with structured context assembly
CORTEX_USE_ASSEMBLER=1 \
DATABASE_URL="postgresql://localhost:5432/cortex_bench" \
python benchmarks/beam/run_benchmark.py --split 100K
```

A.3 Expected Runtimes

A.4 Database Protocol

The benchmark harness creates a fresh `cortex_bench` database per run. Between conversations within a run, all data tables are truncated:

```
TRUNCATE memories, entities, relationships,
entity_memory CASCADE;
```

Table 15: Expected benchmark runtimes.

Configuration	Conversations	Time/Conv	Total
BEAM-100K WRRF	5	~32s	~2.5 min
BEAM-100K Assembler	5	~293s	~24 min
BEAM-10M WRRF	10	~307s	~51 min
BEAM-10M Assembler	10	~733s	~122 min

This ensures zero cross-conversation contamination. The TRUNCATE approach (vs. DROP/CREATE) preserves the schema, extensions, and stored procedures, reducing per-conversation setup time.

A.5 Variance Script

The full variance analysis is run via:

```
bash benchmarks/beam/variance/bench_variance.sh
```

This script runs each configuration 3 times, with PostgreSQL restart between runs, and reports mean and standard deviation of MRR. Observed variance: ± 0.01 MRR.

B Full Ablation Results

B.1 Per-Ability Ablation on BEAM-100K (5 Conversations)

See Table 9 in Section 5.4 for the full per-ability breakdown.

B.2 Configuration Descriptions

- **WRRF**: flat retrieval over the entire corpus, no assembler. Standard top- k selection after WRRF fusion + FlashRank reranking.
- **No Submod**: assembler enabled with stage-scoping, but Phase 1 uses naive top- k selection instead of submodular coverage. Isolates the effect of stage-scoping without diversity.
- **Ph1 Only**: assembler with submodular coverage selection in Phase 1, but Phase 2 (PPR traversal) disabled.
- **Ph1+Ph2**: assembler with submodular coverage in Phase 1 and PPR traversal in Phase 2. Phase 3 is a stub.
- **Full**: same as Ph1+Ph2 in the current implementation (Phase 3 not yet wired to real summaries).

B.3 Key Ablation Findings

1. **Stage-scoping without diversity hurts** (-0.079 vs. WRRF). The No Submod configuration reduces the candidate pool to one stage’s memories and then picks the top- k by score, which selects redundant memories.

2. **Submodular selection alone (Ph1 Only) is not sufficient** (-0.078 vs. WRRF). Without Phase 2 PPR bridging, the assembler is limited to same-stage memories.
3. **The combination of submodular + PPR recovers and slightly exceeds WRRF** ($+0.011$). Neither mechanism alone helps at 100K; together, they produce a marginal improvement.
4. **At 10M, we expect both effects to be amplified**, based on the scale-dependent analysis in Section 5.3.

C Implementation Architecture

C.1 Module Structure

The context assembly module resides in `mcp_server/core/context_assembly/` within the Cortex codebase:

Table 16: Module structure of the context assembly implementation.

Module	Lines	Purpose	Paper Backing
<code>decomposer.py</code>	195	Priority-budgeted assembly	Novel
<code>stage_assembler.py</code>	320	Three-phase assembler	Novel composition
<code>coverage.py</code>	128	Submodular selection (Ph1)	Krause & Guestrin
<code>ppr_traversal.py</code>	177	PPR traversal (Ph2)	Gutierrez et al.
<code>stage_detector.py</code>	196	Pluggable stage detection	Novel interface
<code>condensers.py</code>	277	Domain-aware condensers	Novel
<code>budget.py</code>	123	Token estimation/allocation	Ported from Swift
<code>warning.py</code>	62	Truncation warning banner	Novel
<code>active_retrieval.py</code>	189	Query reformulation	Wang & Chen

Total: $\sim 1,667$ lines of Python across 10 modules.

C.2 Architectural Invariants

All modules are in the `core/` layer (pure business logic, zero I/O). This is enforced by Cortex’s clean architecture: `core/` modules import only from `shared/` and Python stdlib. External dependencies (PostgreSQL queries, embedding generation, schema engine) are injected as callbacks at construction time. Handlers (the composition root layer) wire `core/` to `infrastructure/` via dependency injection.

This means the context assembly logic can be tested entirely in memory with mock callbacks, without a running database. The test suite includes 47 tests covering all modules.

C.3 Callback Interface

The `StageAwareContextAssembler` receives five callbacks:

- `retrieve_fn(query, stage_id, max_results)`: Phase 1 retrieval. Wired to the WRRF pipeline with a stage filter.
- `entity_graph_fn()`: returns (entities, relationships) for PPR. Wired to PostgreSQL entity/relationship queries.

- `memories_by_entity_fn(entity_ids)`: returns memories containing the given entities. Wired to the `entity_memory` junction table.
- `stage_summary_fn(stage_id)`: returns a summary for the given stage. Currently a stub returning empty string.

This callback design ensures that the assembler is agnostic to the underlying storage and retrieval infrastructure.

D BEAM-100K Full Results (20 Conversations, WRRF Control)

For completeness, we include the full WRRF results on the BEAM-100K 20-conversation split (all conversations, not just the 5 used for A/B comparison):

Table 17: BEAM-100K full WRRF results (20 conversations).

Ability	MRR	R@5	R@10	Qs
contradiction_resolution	0.729	90.0%	90.0%	40
temporal_reasoning	0.684	75.0%	80.0%	40
knowledge_update	0.735	87.5%	90.0%	40
multi_session_reasoning	0.596	77.5%	80.0%	40
event_ordering	0.311	50.0%	62.5%	40
summarization	0.315	44.4%	61.1%	36
preference_following	0.309	52.5%	60.0%	39
instruction_following	0.219	27.5%	42.5%	40
abstention	0.125	12.5%	12.5%	40
Overall	0.438	—	—	395

This 20-conversation result (0.438 MRR) is lower than the 5-conversation result (0.591 MRR), reflecting variance across conversations. The 5 conversations selected for A/B comparison happen to be above-average in difficulty.

E Development Timeline and Intermediate Results

E.1 Intermediate BEAM-10M Runs

During development, several intermediate assembler configurations were benchmarked on BEAM-10M:

Table 18: Intermediate BEAM-10M results during development.

Configuration	MRR	Issue
First run (entity_ids bug)	0.100	Phase 2 returned 0 results
After entity_ids fix	0.120	Stage detection used local turn IDs
After stage fix (oracle labels)	0.429	Correct stage assignment
Temporal detector replaces oracle	0.471	Label-free (§6.3)

The jump from 0.120 to 0.429 upon fixing the stage detection confirms that correct stage assignment is critical to the architecture’s performance.

E.2 Debugging the `entity_ids` Bug

The initial Phase 2 implementation consistently returned zero cross-stage memories. The debugging trace: (1) PPR returned non-zero scores for entities, but `memories_by_entity_fn` returned empty lists. (2) The retrieval query’s SELECT clause did not include `entity_ids`. (3) The field was populated at ingest time but not JOINed at retrieval time. (4) Fix: add LEFT JOIN and ARRAY_AGG.

E.3 Debugging the Stage Detection Bug

BEAM-10M turn IDs are plan-relative (each plan restarts numbering from 0), but gold annotations reference global turn indices. Without cumulative plan offsets, the stage detector assigned all memories to “plan-0.” Fix: compute cumulative turn offsets per plan and apply before gold matching.

F Pseudocode for Core Algorithms

F.1 assemble_prompt (ContextDecomposer)

Algorithm 3 ContextDecomposer prompt assembly

Require: template, placeholders, context_window, headroom

```
1: budget  $\leftarrow \lfloor \text{context\_window} \times \text{headroom} \rfloor$ 
2: shell  $\leftarrow \text{substitute}(\text{template}, \{p.\text{key} : \text{""} \mid p \in \text{placeholders}\})$ 
3: variable_budget  $\leftarrow \max(300, \text{budget} - \tau(\text{shell}))$ 
4: {Fast path}
5: if  $\sum_p \tau(p.\text{value}) \leq \text{variable\_budget}$  then
6:   return fill_template(template, placeholders)
7: end if
8: {Progressive condensation}
9: sorted_ph  $\leftarrow \text{sort}(\text{placeholders}, \text{by priority DESC})$ 
10: remaining  $\leftarrow \text{variable\_budget}$ 
11: effective  $\leftarrow \{\}$ 
12: for  $i, p$  in enumerate(sorted_ph) do
13:   not_yet  $\leftarrow |\text{sorted\_ph}| - i$ 
14:   share  $\leftarrow \max(50, \lfloor \text{remaining} / \max(1, \text{not\_yet}) \rfloor)$ 
15:   if  $\tau(p.\text{value}) \leq \text{share}$  then
16:     effective[p.key]  $\leftarrow p.\text{value}$ 
17:     remaining  $\leftarrow \text{remaining} - \tau(p.\text{value})$ 
18:   else
19:     if  $p.\text{condenser} \neq \text{null}$  then
20:       reduced  $\leftarrow p.\text{condenser}(p.\text{value}, \text{share})$ 
21:     else
22:       reduced  $\leftarrow \text{truncate}(p.\text{value}, \text{share})$ 
23:     end if
24:     effective[p.key]  $\leftarrow \text{reduced}$ 
25:     remaining  $\leftarrow \text{remaining} - \min(\tau(\text{reduced}), \text{remaining})$ 
26:   end if
27: end for
28: {Post-assembly safety}
29: prompt  $\leftarrow \text{fill\_template}(\text{template}, \text{effective})$ 
30: while  $\tau(\text{prompt}) > \text{context\_window} - \text{safety\_margin}$  do
31:   halve_lowest_priority(effective, sorted_ph)
32:   prompt  $\leftarrow \text{fill\_template}(\text{template}, \text{effective})$ 
33: end while
34: {Truncation warning}
35: banner  $\leftarrow \text{build\_truncation\_banner}(\text{original}, \text{final})$ 
36: if banner  $\neq \text{""} \text{ then}$ 
37:   prompt  $\leftarrow \text{banner} + \text{"\n\n"} + \text{prompt}$ 
38: end if
39: return prompt
```

F.2 assemble (StageAwareContextAssembler)

Algorithm 4 StageAwareContextAssembler

Require: query, current_stage, budget_split, max_chunks

- 1: {Phase 1: Own-stage}
 - 2: candidates \leftarrow retrieve(query, current_stage, max_chunks \times 3)
 - 3: phase1 \leftarrow submodular_select(candidates, max_chunks, $\lambda = 0.5$)
 - 4: {Phase 2: Cross-stage via PPR}
 - 5: seed_entities \leftarrow extract_entities(phase1)
 - 6: entities, relationships \leftarrow entity_graph()
 - 7: adjacency \leftarrow build_adjacency(entities, relationships)
 - 8: ppr \leftarrow PPR(adjacency, seed_entities, $\alpha = 0.15$)
 - 9: top_entities \leftarrow top_k(ppr, 50)
 - 10: cross \leftarrow memories_by_entities(top_entities)
 - 11: cross \leftarrow filter(cross, stage \neq current_stage)
 - 12: phase2 \leftarrow score_by_ppr(cross, ppr)[:max_chunks]
 - 13: {Phase 3: Summary fallback}
 - 14: covered \leftarrow {current_stage} \cup stages_of(phase2)
 - 15: uncovered \leftarrow all_stages $-$ covered
 - 16: phase3 \leftarrow [stage_summary(s) for s in uncovered]
 - 17: **return** structured_context(phase1, phase2, phase3)
-

References

- Kevin Beyer, Jonathan Goldstein, Raghu Ramakrishnan, and Uri Shaft. When is “nearest neighbor” meaningful? In *Proceedings of the 7th International Conference on Database Theory (ICDT)*, pages 217–235, 1999.
- Sergey Brin and Lawrence Page. The anatomy of a large-scale hypertextual web search engine. *Computer Networks and ISDN Systems*, 30(1–7):107–117, 1998. doi: 10.1016/S0169-7552(98)00110-X.
- Jaime Carbonell and Jade Goldstein. The use of MMR, diversity-based reranking for reordering documents and producing summaries. In *Proceedings of the 21st Annual International ACM SIGIR Conference*, pages 335–336, 1998. doi: 10.1145/290941.291025.
- Deshraj Chheda et al. mem0: The memory layer for AI agents. *arXiv preprint*, 2024.
- Allan M. Collins and Elizabeth F. Loftus. A spreading-activation theory of semantic processing. *Psychological Review*, 82(6):407–428, 1975. doi: 10.1037/0033-295X.82.6.407.
- Gordon V. Cormack, Charles L. A. Clarke, and Stefan Buettcher. Reciprocal rank fusion outperforms Condorcet and individual rank learning methods. In *Proceedings of the 32nd International ACM SIGIR Conference*, pages 758–759, 2009. doi: 10.1145/1571941.1572114.
- Bernal Jiménez Gutierrez, Yiheng Shu, Yu Gu, Michihiro Yasunaga, and Yu Su. HippoRAG: Neurobiologically inspired long-term memory for large language models. In *Advances in Neural Information Processing Systems (NeurIPS)*, 2024.

- Jina AI. Late chunking: Contextual chunk embeddings using long-context embedding models, 2025. Technical Report.
- Vladimir Karpukhin, Barlas Oguz, Sewon Min, Patrick Lewis, Ledell Wu, Sergey Edunov, Danqi Chen, and Wen-tau Yih. Dense passage retrieval for open-domain question answering. In *Proceedings of the 2020 Conference on Empirical Methods in Natural Language Processing (EMNLP)*, pages 6769–6781, 2020. doi: 10.18653/v1/2020.emnlp-main.550.
- Omar Khattab and Matei Zaharia. ColBERT: Efficient and effective passage search via contextualized late interaction over BERT. In *Proceedings of the 43rd International ACM SIGIR Conference*, pages 39–48, 2020. doi: 10.1145/3397271.3401075.
- Andreas Krause and Carlos Guestrin. Near-optimal sensor placements in Gaussian processes. *Journal of Machine Learning Research*, 9:235–284, 2008.
- Amy N. Langville and Carl D. Meyer. A survey of eigenvector methods for web information retrieval. *SIAM Review*, 47(1):135–161, 2005. doi: 10.1137/S0036144503424786.
- Kasper Green Larsen and Jelani Nelson. Optimality of the Johnson-Lindenstrauss lemma. In *Proceedings of the 58th Annual IEEE Symposium on Foundations of Computer Science (FOCS)*, pages 633–638, 2017. doi: 10.1109/FOCS.2017.64.
- Hui Lin and Jeff Bilmes. A class of submodular functions for document summarization. In *Proceedings of the 49th Annual Meeting of the Association for Computational Linguistics (ACL)*, pages 510–520, 2011.
- Adyasha Maharana et al. LoCoMo: Long-context conversation memory benchmark. In *Proceedings of the 62nd Annual Meeting of the Association for Computational Linguistics (ACL)*, 2024.
- James L. McClelland, Bruce L. McNaughton, and Randall C. O’Reilly. Why there are complementary learning systems in the hippocampus and neocortex. *Psychological Review*, 102(3):419–457, 1995. doi: 10.1037/0033-295X.102.3.419.
- Michel Minoux. Accelerated greedy algorithms for maximizing submodular set functions. In *Optimization Techniques*, volume 7 of *Lecture Notes in Control and Information Sciences*, pages 234–243. 1978.
- Niklas Muennighoff et al. MTEB: Massive text embedding benchmark. In *Proceedings of the 17th Conference of the European Chapter of the Association for Computational Linguistics (EACL)*, pages 2014–2037, 2023.
- Charles Packer et al. Letta: An operating system for AI agents with long-term memory. *arXiv preprint*, 2024.
- Miloš Radovanović, Alexandros Nanopoulos, and Mirjana Ivanović. Hubs in space: Popular nearest neighbors in high-dimensional data. *Journal of Machine Learning Research*, 11:2487–2531, 2010.
- Nils Reimers and Iryna Gurevych. Sentence-BERT: Sentence embeddings using Siamese BERT-networks. In *Proceedings of the 2019 Conference on Empirical Methods in Natural Language Processing (EMNLP)*, pages 3982–3992, 2019. doi: 10.18653/v1/D19-1410.
- Parth Sarthi et al. RAPTOR: Recursive abstractive processing for tree-organized retrieval. In *Proceedings of the International Conference on Learning Representations (ICLR)*, 2024.

- Hanne Stensola, Tor Stensola, Trygve Solstad, Kristian Frøland, May-Britt Moser, and Edvard I. Moser. The entorhinal grid map is discretized. *Nature*, 492:72–78, 2012. doi: 10.1038/nature11649.
- Arash Tavakoli et al. BEAM: Beyond a million tokens — benchmarking long-term memory in AI agents. In *Proceedings of the International Conference on Learning Representations (ICLR)*, 2026.
- Timothy J. Teyler and Jerry W. Rudy. The hippocampal indexing theory and episodic memory: Updating the index. *Hippocampus*, 17(12):1158–1169, 2007. doi: 10.1002/hipo.20350.
- Nandan Thakur, Nils Reimers, Andreas Rücklé, Abhishek Srivastava, and Iryna Gurevych. BEIR: A heterogeneous benchmark for zero-shot evaluation of information retrieval models. In *Advances in Neural Information Processing Systems (NeurIPS)*, 2021.
- Dorothy Tse, Rosamund F. Langston, Masaki Takeyama, Ingrid Betsus, Patrick A. Spooner, Emma R. Wood, Menno P. Witter, and Richard G. M. Morris. Schemas and memory consolidation. *Science*, 316(5821):76–82, 2007. doi: 10.1126/science.1135935.
- Cheng Wang and Jian Chen. MIRIX: Multi-agent memory system for LLM-based agents. *arXiv preprint*, 2025.
- Yucheng Wu et al. LongMemEval: Benchmarking long-term memory in AI assistants. In *Proceedings of the International Conference on Learning Representations (ICLR)*, 2025.
- Boyuan Xu et al. A-MEM: Agentic memory for LLM agents. In *Advances in Neural Information Processing Systems (NeurIPS)*, 2025.
- Dawei Zhu et al. LongEmbed: Extending embedding models for long context retrieval. *arXiv preprint*, 2024.